Enhancement of Power-Added Efficiency in GaAs Power Amplifiers by Dynamic Gate Biasing

Enhancement of Power-Added Efficiency in GaAs Power Amplifiers by Dynamic Gate Biasing

Göksu Kaval[#*1], Gregor Lasser[*2], Marcus Gavell[#3], and Christian Fager[*4]
[#]Gotmic AB, Sweden
[*]Microwave Electronics Laboratory, Chalmers University of Technology, Sweden
{[1]goksu.kaval, [3]marcus.gavell}@gotmic.se, {[2]gregor.lasser, [4]christian.fager}@chalmers.se

***Abstract* — We demonstrate the efficiency and linearity improvement of an E-band GaAs power amplifier (PA) through dynamic gate modulation. By optimizing the coefficients of the linear power tracking gate modulation function, we enhance the output power at the spectrum emission mask limit from $24.1\,\mathrm{dBm}$ to $25.8\,\mathrm{dBm}$. This leads to a significant improvement in average power-added efficiency ($\overline{PAE}$) from 4.9% to 7.4%, surpassing third-order digital pre-distortion (DPD). Our findings highlight the potential of dynamic gate biasing for enhancing efficiency and linearity in mm-wave and sub-THz power amplifiers.**

***Keywords* — power amplifiers, dynamic gate biasing, power tracking.**

I. Introduction

To support high data rates and spectral efficiency, telecommunication systems employ high-order modulation schemes. These modulation formats result in signals with large dynamic range and high peak-to-average power ratio. However, power amplifiers (PAs) at the transmitter front ends typically exhibit nonlinear gain characteristics. The non-linearity of PAs results in spectrum regrowth, which imposes limitations on the maximum RF output power due to strict spectrum mask requirements for point-to-point back-haul systems. Additionally, it is well-known that PA efficiency, particularly at mm-wave/sub-THz frequencies drops drastically at output power back off. These challenges highlight the potential of dynamic gate biasing, which can reduce dc power consumption at output power back off and provide greater supply current to maintain linear gain at high power levels allowing the PA to operate at more efficient region with modulated signals.

The potential improvement in adjacent channel leakage ratio (ACLR) through dynamic biasing was discussed in [1]. Additionally, dynamic gate biasing techniques were employed for auxiliary amplifiers in Doherty power amplifier designs, as presented in [2]. The effectiveness of dynamic gate biasing in linearizing GaN HEMT PAs was investigated in [3].In [4], more than one stage's gates of a GaN PA were dynamically biased to improve linearity for targeted gain and output power. Furthermore, [5] examined the trade-off between PAE and linearity in gate-modulated PAs based on simulations. In this paper, our objective is to experimentally demonstrate the enhancement of average output power and efficiency of an E-Band GaAs HEMT MMIC PA while complying with the spectrum emission mask limit through the implementation of dynamic gate biasing.

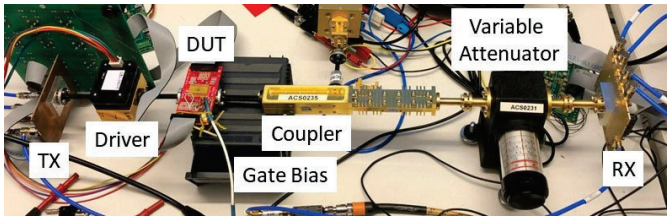

Fig. 1. Key components of the modulated signal measurement setup.

II. Measurement Setup

A measurement setup has been developed to drive the RF and gate input terminals of an E-band PA with modulated signals and gradually increase the average RF_{out} power ($\overline{P_{\mathrm{out}}}$) until the output spectrum reaches the ETSI EN 302-217-2 spurious emission mask limit. At this power limit, the average power added efficiency ($\overline{PAE}$) of the PA is measured. This procedure was repeated with different gate modulation functions and the optimum power tracking coefficients that maximize both $\overline{PAE}$ and $\overline{P_{\mathrm{out}}}$ were found.

The measurement setup, presented with a block diagram in Fig. 2, was constructed using commercially available E-band telecommunication components, as shown in Fig. 1. The desired complex baseband equivalent representation of the signal at the output of the PA ($y_{\mathrm{d}}(n)$) was generated by modulating a bit sequence using QAM16 modulation. Iterative learning architecture (ILA)-based calibration techniques were utilized to compensate for TX I/Q imbalance and scale the signal, while pre-determined calibration coefficients were applied for LO leakage cancellation. The signal was up-converted to $80\,\mathrm{GHz}$ using an E-Band TX module. To ensure linear operation, a gAPZ0092 driver amplifier with a gain of $16\,\mathrm{dB}$ was inserted between the DUT PA and the transmitter.

The DUT is a 1W PA with $16\,\mathrm{dB}$ gain, designed in the WIN Semiconductor's PP10-10 $100\,\mathrm{nm}$ GaAs process. As shown in Fig. 2, the gate bias voltage of the DUT's final stage is dynamically modulated based on the expected instantaneous output power of the PA, calculated using $y_{\mathrm{d}}(n)$. First-order power tracking is employed to limit the bandwidth of the gate drive function [6]. We, therefore, can express

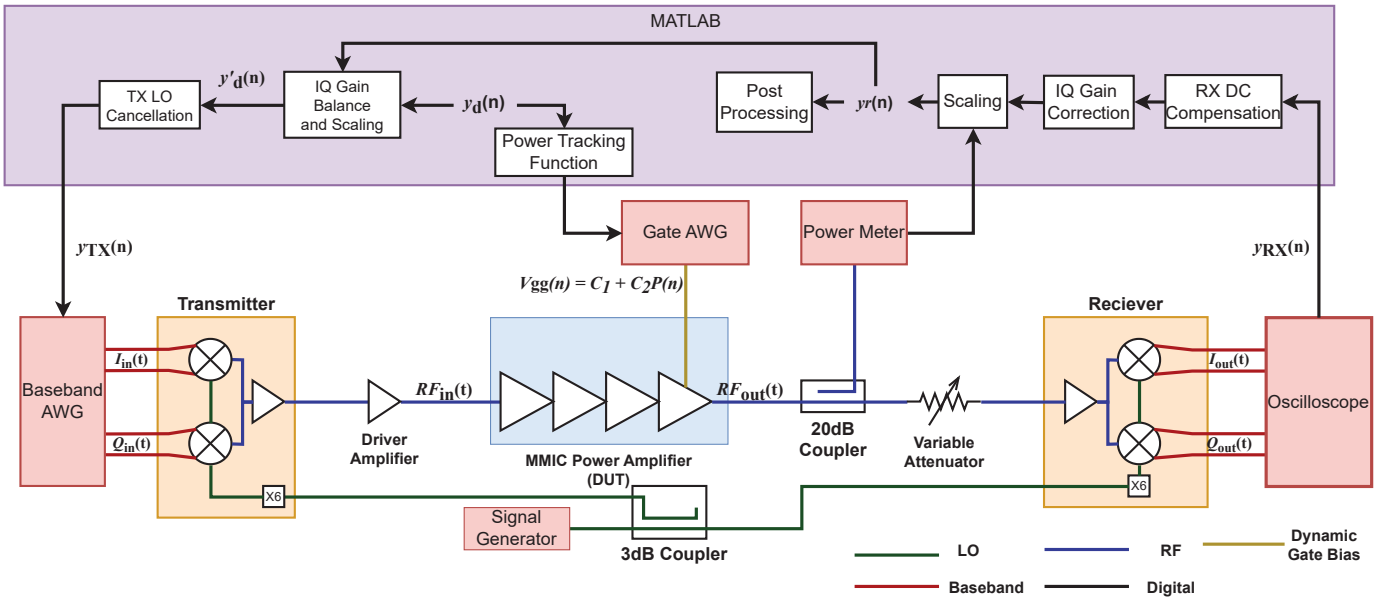

Fig. 2. Block diagram of the measurement setup.

the band-limited gate bias voltage ($V_{gg}(n)$) as a polynomial function of instantaneous output power ($P(n)$) as

$$V_{gg}(n) = C_1 + C_2 P(n). \tag{1}$$

On the receiver side, the gMRX00014 E-Band receiver (RX) was utilized to down-convert the RF signal to the baseband. To ensure linear operation, an RF attenuator was inserted at the input of the down-converting receiver. The down-converted signal was then captured by an oscilloscope, yielding the sampled complex time-domain signal $y_{\mathrm{RX}}(n)$.

The received baseband signal underwent LO leakage cancellation and IQ gain imbalance correction based on pre-determined factors. Scaling the baseband signal using the power meter reading yielded $y_{\mathrm{r}}(n)$, which is the correctly voltage-scaled baseband equivalent of $RF_{\mathrm{out}}(t)$.

Finally, $y_{\mathrm{r}}(n)$ was subjected to post-processing analysis to monitor the quality of the data transmission. This analysis included calculations of the output spectrum, constellation diagrams, error vector magnitude (EVM), and other relevant metrics.

III. Characterization and Modeling of Power Amplifier

Initially, the DUT PA was disconnected to measure a reference case, and the input power of the TX was varied. Power meter readings were used to record the output power after the driver amplifier. The phase of the RF signal was obtained from the phase of $Q_{\mathrm{Out}} + jI_{\mathrm{Out}}$.

Then, the DUT PA was connected, and the same sweeps were repeated with different static gate bias voltage settings. The measured output power, RF phase, and DC power consumption were recorded. In combination with the reference case, this enabled the characterization of the PA's AM/AM, AM/PM, and DC power response at different gate bias levels, which is known as continuous-wave (CW) characterization. During CW characterization, RF frequency were kept constant. Therefore, the characterization does not capture memory effects.

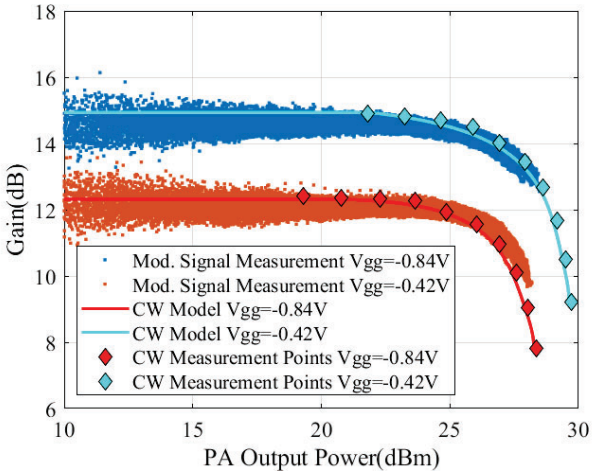

Fig. 3. Gain of the PA measured with CW and modulated signals and modelled gain based on CW measurement

The PA's complex RF output voltage and power consumption were modeled using memoryless polynomial functions of the gate bias voltage and input RF voltage through CW characterization. Polynomial coefficients were determined by least squares fitting. Fig. 3 shows a very good agreement between the gain response obtained from CW measurements, the polynomial model, and the gain with 62.5 MHz wide modulated signals.

IV. Finding The Optimum Gate Functions and Measurements

Utilizing the PA model described in Section III, we initially investigate various gate power tracking functions in a simulation environment similar to the one described in [7] to optimize $\overline{PAE}$ and $\overline{P_{\text{out}}}$ within the spectrum mask emission limit. The simulation entails modulating a binary sequence using QAM16 modulation with a symbol rate of $50\,\text{Msymbol/s}$ and filtering it with a root-raised cosine filter with a roll-off factor of 0.25. The power level of the signal is progressively increased until the output waveform's spectrum breaches the spectrum emission mask for $62.5\,\text{MHz}$ bandwidth signals. At this limit, we record performance metrics such as $\overline{PAE}$ and $\overline{P_{\text{out}}}$. Figures 4a and 4b demonstrate the simulated enhancement in $\overline{PAE}$ and $\overline{P_{\text{out}}}$ at the mask limit for specific power tracking coefficients.

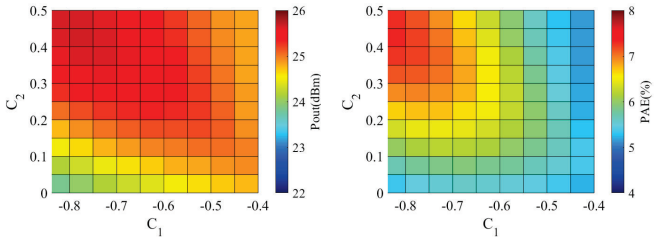

(a) (b)

Fig. 4. Simulated (a) $\overline{P_{\text{out}}}$, (b) $\overline{PAE}$ at ETSI spectrum mask limit with different power tracking coefficients

The power tracking coefficients determined by simulations were tested on the measurement setup with an $80\,\text{GHz}$ carrier frequency. Due to limitations in the evaluation board and on-chip biasing network, a $1.25\,\text{MHz}$ wide QAM-16 signal was used instead of aimed $62.5\,\text{MHz}$ channel bandwidth and the mask scaled accordingly. Reasonable agreement between simulation and measurements was observed, when comparing the results in Fig. 4 and Fig. 5, respectively.

The experimental results demonstrated that the most efficient static biasing case $(C_1 = -0.53, C_2 = 0)$ achieved a $\overline{PAE}$ of 4.8%. However, the best linear power tracking case $(C_1 = -0.78, C_2 = 0.38)$ significantly improved the $\overline{PAE}$ to 7.4%. Additionally, this power tracking function enhanced $\overline{P_{\text{out}}}$ to $25.8\,\text{dBm}$, compared to the case with the highest $\overline{P_{\text{out}}}$ at the mask limit $(C_1 = -0.84, C_2 = 0)$. The normalized AM/AM and AM/PM responses of the amplifier for the power tracking and static bias case, which achieved the highest $\overline{P_{\text{out}}}$ at the mask limit, are presented in Fig. 6a and Fig. 6b.

For the sake of comparison, we also included results for a third-order digital pre-distortion (DPD) linearization case, applied to the static bias case giving the highest $\overline{P_{\text{out}}}$. The results for all cases tested are summarized in Table 1. According to the results, linear power tracking-based dynamic biasing granted better improvement compared to the 3^{rd} order DPD.

Fig. 7 compares the output spectrum of the PA for different cases: static bias with the highest $\overline{P_{\text{out}}}$, linear power

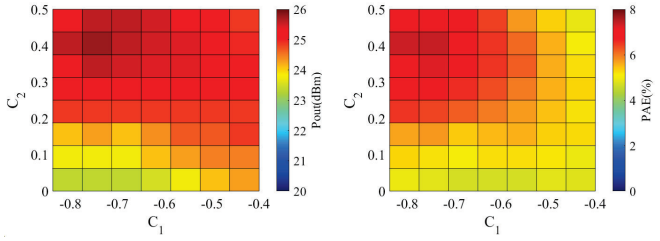

(a) (b)

Fig. 5. Measured (a) $\overline{P_{\text{out}}}$, (b) $\overline{PAE}$ at ETSI spectrum mask limit with different power tracking coefficients

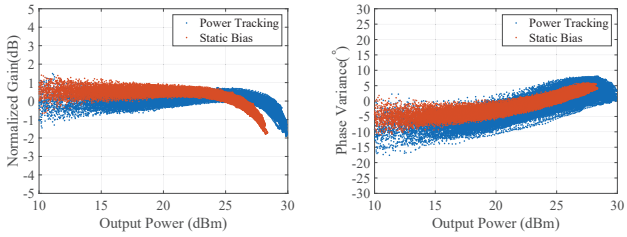

(a) (b)

Fig. 6. Measured (a) AM/AM, (b) AM/PM response of the PA at the mask limit for static and dynamic gate bias

Table 1. Measurement results at spectrum mask limit

	C_1	C_2	$\overline{PAE}$	$\overline{P_{\text{out}}}$	$\overline{Gain}$
Best $\overline{P_{\text{out}}}$ Static	-0.53	0	4.8	24.1	14.0
Best $\overline{PAE}$ Static	-0.84	0	4.9	23.4	12.07
Linear Power Tracking	-0.78	0.38	7.4	25.8	13.2
3^{rd} Order DPD	-0.53	0	5.5	24.8	13.3

$\overline{PAE}$ in %, $\overline{P_{\text{out}}}$ in dBm, $\overline{Gain}$ is in dB

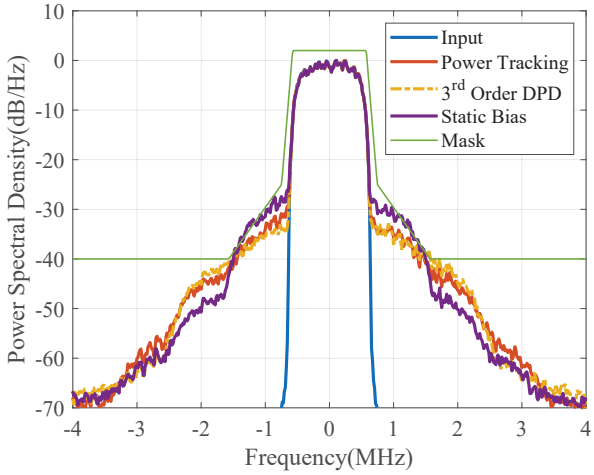

Fig. 7. Comparison of the measured spectrum at $25.2\,\text{dBm}$ $\overline{P_{\text{out}}}$.

tracking, and static bias with DPD at $25.2\,\mathrm{dBm}$ $\overline{P_{\mathrm{out}}}$. The results demonstrate that linear power tracking achieves similar spectral regrowth suppression characteristics as the 3^{rd} order DPD, highlighting its effectiveness in not only linearizing but also enhancing their efficiency.

Conclusion

This work demonstrates the experimental enhancement of efficiency and output power of an E-band GaAs MMIC PA through linear power tracking-based gate bias modulation. The implementation of a gate bias signal based on linear power tracking results in an increase in $\overline{PAE}$ from 4.8% to 7.4%, as well as an improvement in $\overline{P_{\mathrm{out}}}$ to $25.8\,\mathrm{dBm}$ from $24.1\,\mathrm{dBm}$ compared to static bias settings. Furthermore, dynamic gate biasing surpasses the performance of a 3rd order DPD technique in our experiments. The bandwidth limitations of the current gate bias will be addressed in future PA designs, enabling the extension of these promising results to commercial backhaul link applications.

Acknowledgment

This work is supported by the Swedish Innovation Agency grant ENTRY100GHz with grant number 2020-02889 under the Eureka CELTIC framework.

References

[1] Y. Noh and C. Park, "An intelligent power amplifier MMIC using a new adaptive bias control circuit for W-CDMA applications," *IEEE Journal of Solid-State Circuits*, vol. 39, no. 6, pp. 967–970, 2004.

[2] K. Onizuka, K. Ikeuchi, S. Saigusa, and S. Otaka, "A 2.4 GHz CMOS doherty power amplifier with dynamic biasing scheme," in *2012 IEEE Asian Solid State Circuits Conference (A-SSCC)*, 2012, pp. 93–96.

[3] D. Gecan, M. Olavsbraten, and K. M. Gjertsen, "Comprehensive investigation of a dynamic gate biasing technique for linearity improvement based on measurement of a 10 W GaN HEMT power amplifier," in *2016 24th Telecommunications Forum (TELFOR)*, 2016, pp. 1–3.

[4] G. Lasser, M. R. Duffy, and Z. Popović, "Dynamic dual-gate bias modulation for linearization of a high-efficiency multistage PA," *IEEE Transactions on Microwave Theory and Techniques*, vol. 67, no. 7, pp. 2483–2494, 2019.

[5] G. Kaval, G. Lasser, M. Gavell, and C. Fager, "Multi-stage gate modulation of E-band MMIC power amplifier for efficiency improvement," in *2022 International Workshop on Integrated Nonlinear Microwave and Millimetre-Wave Circuits (INMMiC)*, 2022, pp. 1–3.

[6] M. Olavsbråten and D. Gecan, "Bandwidth reduction for supply modulated RF PAs using power envelope tracking," *IEEE Microwave and Wireless Components Letters*, vol. 27, no. 4, pp. 374–376, 2017.

[7] H. V. Hunerli, M. Gavell, P. Taghikhani, and C. Fager, "A methodology for analysis of mm-wave transmitter linearization trade-offs under spectrum constraints," in *2018 International Workshop on Integrated Nonlinear Microwave and Millimetre-wave Circuits (INMMIC)*, 2018, pp. 1–3.